catalysts

MDPI

Article

Application of Platinum Nanoparticles Decorating Mesoporous Carbon Derived from Sustainable Source for Hydrogen Evolution Reaction

Erik Biehler [1,2], Qui Quach [1,2] and Tarek M. Abdel-Fattah [1,2,*]

[1] Applied Research Center at Thomas Jefferson National Accelerator Facility, 12000 Jefferson Avenue, Newport News, VA 23606, USA; erik.biehler@cnu.edu (E.B.); qui.quach.13@cnu.edu (Q.Q.)
[2] Department of Molecular Biology and Chemistry, Christopher Newport University, 1 Avenue of the Arts, Newport News, VA 23606, USA
* Correspondence: fattah@cnu.edu

Abstract: The perpetually fluctuating economic and environmental climate significantly increases the demand for alternative fuel sources. The utilization of hydrogen gas is a viable option for such a fuel source. Hydrogen is one of the most energy-dense known substances; however, it is unfortunately also highly volatile, especially in the diatomic gaseous state most commonly used to store it. The utilization of a hydrogen feedstock material such as sodium borohydride ($NaBH_4$) may prove to mitigate this danger. When $NaBH_4$ reacts with water, hydrogen stored within its chemical structure is released. However, the rate of hydrogen release is slow and thus necessitates a catalyst. Platinum nanoparticles were chosen to act as a catalyst for the reaction, and to prevent them from conglomerating, they were embedded in a backbone of mesoporous carbon material (MCM) derived from a sustainable corn starch source. The nanocomposite (Pt-MCM) was characterized via transmission electron microscopy (TEM), scanning electron microscopy (SEM), energy-dispersive X-ray spectroscopy (EDS), and X-ray diffraction (XRD). Pt-MCM underwent catalytic testing, revealing that the catalytic activity of the Pt-MCM composite catalysts increased with increasing quantities of sodium borohydride, lower pH levels, and higher temperatures. The activation energy of the catalyzed reaction was found to be 37.7 kJ mol^{-1}. Reusability experiments showed an initial drop off in hydrogen production after the first trial but subsequent stability. This Pt-MCM catalyst's competitive activation energy and sustainable MCM backbone derived from readily available corn starch make it a promising option for optimizing the hydrogen generation reaction of $NaBH_4$.

Keywords: hydrogen evolution; mesoporous carbon; platinum nanoparticles; sustainable source; hydrogen production; nanocomposite

check for updates

Citation: Biehler, E.; Quach, Q.; Abdel-Fattah, T.M. Application of Platinum Nanoparticles Decorating Mesoporous Carbon Derived from Sustainable Source for Hydrogen Evolution Reaction. *Catalysts* **2024**, *14*, 423. https://doi.org/10.3390/catal14070423

Academic Editors: Vincenzo Vaiano and Olga Sacco

Received: 25 May 2024
Revised: 18 June 2024
Accepted: 20 June 2024
Published: 2 July 2024

Copyright: © 2024 by the authors. Licensee MDPI, Basel, Switzerland. This article is an open access article distributed under the terms and conditions of the Creative Commons Attribution (CC BY) license (https://creativecommons.org/licenses/by/4.0/).

1. Introduction

Overdependence on non-renewable energy sources is a growing problem worldwide. The global supply of non-renewables will inevitably diminish, which may lead to a global energy crisis. Furthermore, the continued use of fossil fuels, such as oil, coal, and natural gas, causes significant environmental damage through the release of CO_2 and other greenhouse gases. Reports in 2019 showed that atmospheric CO_2 levels were at 415 parts per million, higher than they had ever been in the last 800,000 years [1]. Thus, research into new renewable and clean energy sources is needed. One viable method of clean energy production is through the use of hydrogen as a fuel. Hydrogen is one of the most abundant substances on earth and releases nearly three times the amount of energy per kilogram compared with gasoline when used in fuel cells [2]. However, one of the main storage methods of hydrogen is a compressed gas that is dangerous due to the possibility of combustion [3]. This danger can be mitigated through the hydrogen evolution reaction (HER). This reaction is known for producing high-quality hydrogen gas from

water; however, a catalyst is typically required for optimization [4]. A number of different materials have been explored for HERs, including platinum and ruthenium [5–8]. This reaction, involving the hydrolysis of a hydrogen feedstock material, produces hydrogen gas as seen in the following Equation (1). This hydrogen gas can then be applied in hydrogen fuel cells to generate energy.

$$NaBH_4 + 2H_2O \rightarrow NaBO_2 + 4H_2(\Delta H < 0) \quad (1)$$

When it comes to hydrogen feedstock materials, boron hydrides are highly sought after for their hydrogen storage ability. Two materials, sodium borohydride ($NaBH_4$) and ammonia borane (NH_3BH_3), have garnered a lot of attention due to their weight percentages of hydrogen being 10.8% and 19.5%, respectively. Sodium borohydride was chosen as a hydrogen feedstock material for this study as it is more commonly produced and cheaper to obtain [9].

As mentioned before, the HER proceeds slowly without a catalyst. Rapid development in the field of nanotechnology has yielded effective catalysts that may be used to speed up this reaction. One specific subset of nanomaterials, mesoporous carbon materials (MCMs), is a promising option. MCMs fall under the larger umbrella of porous carbons and are defined as having pore size of 2–50 nm [10,11]. The pores in an MCM create a high surface area, allowing many catalytic reactions to occur simultaneously. Along with having high surface areas, MCMs have shown good electrical, mechanical, and thermal properties [12,13]. MCMs have a variety of applications including use in electrodes, absorbent materials, and, more importantly, catalysis [12–14]. Although MCMs can singlehandedly function as effective catalysis, there is room for improvement. Through the application of metal nanoparticles, an MCM catalyst can be enhanced.

Nanomaterials such as nanofilms and nanoparticles can function as excellent catalysts due to their high surface-area-to-volume ratio [15–19]. Metals that are known to be inert at the bulk state exhibit increased catalytic activity in the nanoparticle size range (1–100 nm) [15]. However, the highly varying properties of nanoparticles, including size, shape, and texture, make it difficult to control nanoparticle stability. In application, nanoparticles tend to agglomerate, creating larger particles, thus resulting in a decrease in catalytic activity [20–22]. In order to resolve this issue, nanoparticles can be embedded in a framework to prevent them from interacting [13]. Due to their high porosity and surface area, MCMs can function as an effective framework. Through the combination of nanoparticles and MCMs, a nanocomposite material is formed. The catalytic nature of both materials can be utilized to their full extent, creating a stronger and more stable catalyst.

Platinum nanoparticles were chosen as the metal portion of the nanocomposite material in this study due to their superior catalytic properties. Platinum is renowned for its high catalytic activity, making it an essential component in various industrial applications [23–25]. One significant application of platinum is as a catalyst for the oxidation of methane. In this process, platinum facilitates the conversion of methane (CH_4) into carbon dioxide (CO_2) and water (H_2O). This reaction is particularly important in natural gas processing and in efforts to mitigate methane, a potent greenhouse gas, from entering the atmosphere. The high efficiency of platinum in promoting this reaction makes it invaluable in environmental protection and energy industries. Platinum is also extensively used in the hydrosilylation reaction, a chemical process that involves the addition of silicon–hydrogen bonds to unsaturated organic compounds. This reaction is crucial in the production of silicones and other organosilicon materials, which are widely used in industries ranging from electronics to medical devices due to their stability and versatility. In the automotive industry, platinum's role as a catalyst in catalytic converters is well established. Catalytic converters are critical components in vehicle exhaust systems designed to reduce harmful emissions. Platinum, along with other precious metals like palladium and rhodium, helps convert toxic gases such as carbon monoxide (CO), hydrocarbons (HC), and nitrogen oxides (NO_x) into less harmful substances like carbon dioxide (CO_2), water (H_2O), and nitrogen (N_2). This conversion is vital for meeting stringent emission standards

and reducing the environmental impact of vehicles. The choice of platinum nanoparticles enhances these catalytic processes due to their increased surface area, which provides more active sites for reactions. This increased surface area significantly boosts the efficiency and effectiveness of platinum as a catalyst. Thus, incorporating platinum nanoparticles into a nanocomposite material leverages these benefits, making the material highly efficient for catalytic applications. This choice underscores the importance of platinum in advancing both traditional industrial processes and cutting-edge technologies, ensuring better performance, sustainability, and environmental protection. In the form of nanoparticles, platinum exhibits enhanced catalytic properties due to its increased surface area, which provides more active sites for reactions. This makes platinum nanoparticles particularly effective in several advanced catalytic applications. For instance, they are employed as catalysts for the hydrogenation of alkynes, a crucial reaction in the synthesis of various fine chemicals and pharmaceuticals. Furthermore, platinum nanoparticles are integral to the functioning of proton exchange membrane (PEM) fuel cells, where they catalyze the hydrogen oxidation reaction at the anode and the oxygen reduction reaction at the cathode, thus enabling efficient energy conversion in hydrogen fuel cells. Additionally, platinum nanoparticles are utilized in the oxygen evolution reaction (OER), a key reaction in electrochemical water splitting and renewable energy storage systems. The versatility and efficiency of platinum nanoparticles in these catalytic processes underscore their importance in both traditional and emerging technologies [23–25].

In the nanoparticle range, platinum has been extensively applied as a catalyst in several advanced and critical chemical processes due to its exceptional catalytic properties. One such application is in the hydrogenation of alkynes [26–28]. This reaction involves the addition of hydrogen to alkyne compounds to produce alkanes or alkenes. Platinum nanoparticles, with their high surface area and enhanced reactivity, serve as highly efficient catalysts for this process. The hydrogenation of alkynes is a crucial step in the synthesis of a wide range of fine chemicals, pharmaceuticals, and specialty materials where the selective conversion of triple bonds to single or double bonds is often required. Moreover, platinum nanoparticles are integral components of proton exchange membrane (PEM) fuel cells, a promising technology for clean energy. In PEM fuel cells, platinum nanoparticles are used as catalysts on both the anode and cathode sides. At the anode, they facilitate the hydrogen oxidation reaction (HOR), where hydrogen molecules are split into protons and electrons. At the cathode, they catalyze the oxygen reduction reaction (ORR), where oxygen molecules combine with protons and electrons to form water. The high catalytic activity of platinum nanoparticles significantly enhances the efficiency of these reactions, thereby improving the overall performance and energy output of PEM fuel cells. This application is particularly important in the development of sustainable and efficient power sources for vehicles, portable electronics, and stationary power generation systems. Additionally, platinum nanoparticles are used as catalysts for the oxygen evolution reaction (OER). The OER is a key half-reaction in electrochemical water splitting, which is a process that generates hydrogen and oxygen from water using an electric current. This reaction is also critical in rechargeable metal–air batteries and other energy storage technologies. Platinum nanoparticles, with their high catalytic activity and stability, play a vital role in enhancing the efficiency of the OER, thereby improving the performance of water splitting systems and energy storage devices. The ability of platinum nanoparticles to effectively catalyze the OER is crucial for advancing renewable energy technologies and achieving a sustainable energy future. The use of platinum nanoparticles in these catalytic processes highlights their versatility and indispensability in both existing and emerging technologies. Their use in the hydrogenation of alkynes, PEM fuel cells, and OERs exemplifies their significant contribution to the fields of chemical synthesis, clean energy production, and renewable energy storage, making them essential materials in the quest for technological and environmental advancements [26–28].

In this work, the synthesis of a nanocomposite material containing platinum nanoparticles embedded in MCMs was performed. The catalytic activity of both substituents of the

nanocomposite material is high, so the combination of both materials may result in a stable and highly effective catalyst. In order to test for catalytic activity, the nanocomposite was applied in the HER using $NaBH_4$ as a feedstock material. To test for optimum conditions, the pH, temperature, and quantity of $NaBH_4$ were varied. Furthermore, the nanocomposite material was characterized using X-ray diffraction, scanning electron microscopy, transmission electron microscopy, and energy-dispersive X-ray spectroscopy.

2. Experimental Section

2.1. Synthesis of Materials

To synthesize the platinum nanoparticles, 100 mL of a 1 mM solution of chloroplatinic acid hydrate (Sigma Aldrich, St. Louis, MO, USA) was brought to a boil, and 5 mL of 1% *w*/*w* aqueous sodium citrate (Sigma Aldrich) was added dropwise with stirring for 5 min until a color change was observed. MCMs can be synthesized from corn starch, as the environmentally friendly corn starch is heated to form a gel, treated with ethanol and organic acid, and then cooked, resulting in the desired MCM material [29]. The final nanocomposite material was formed by combining 40 mL of the platinum nanoparticle solution with 1 g of MCM nanopowder. Incipient wetness impregnation was used to allow the catalyst to attach to the mesoporous carbon structure [16]. After the filtration of the product, the precipitate was dried for 24 h at 100 °C.

2.2. Characterization

The catalyst was characterized using transmission electron microscopy (TEM, JEM-2100F) and scanning electron microscopy (SEM, JEOL JSM-6060LV, JEOL, Akishima, Tokyo, Japan) to visualize nanoparticle and MCM surface interactions. Energy-dispersive X-ray spectroscopy (EDS, ThermoScientific UltraDry, Thermo Fischer Scientific, Waltham, MA, USA) images were taken at different magnifications and at an accelerating voltage of 15 kV. X-ray diffraction (XRD, Rigaku Miniflex II, Cu Kα X-ray, nickel filters, Rigaku, Tokyo, Japan) was utilized to confirm the elemental composition and crystallinity structure of the MCM and Pt-MCM. The acquisition rate for the XRD measurements was 5° min^{-1} with a step size of 0.02°.

3. Catalytic Tests

In order to test the nanocomposite material for its catalytic activity, it was tested under a variety of reaction conditions. First, 0.01 g of a 0.6% Pt loading of each catalyst was combined with 100 mL of deionized (DI) water in a flask with a magnetic stir rod. The gravimetric water displacement system described by Huff et al. (2017) [16] was used to allow for the measurement and recording of the produced hydrogen. An Ohaus Pioneer Balance (Pa124, OHAUS, Parsippany, NJ, USA) and logging software (SPDC Data Collector, OHAUS, Parsippany, NJ, USA, V2.04) were used to record data under differing quantity, temperature and pH conditions. In this system, a series of Buchner flasks were connected with plastic tubing. Both the reactant and catalyst were added to one flask, sealed with a stopper, and stirred via magnetic stirring. As hydrogen filled the first flask, it travelled through plastic tubing into the second flask. The second flask was also filled with 100 mL of DI water and sealed with a rubber stopper. Through this stopper was additional plastic tubing that led to a plastic cub on the mass balance. As the second flask filled with hydrogen gas, the DI water was forced up the tubing and drip into the cup, where the mass of the water could be displaced. The mass of the displaced water was then used to determine the volume of hydrogen produced per trial. The quantities of $NaBH_4$ used were 0.00079 mol, 0.00095 mol and 0.0011 mol; pH trials were conducted at solution pH levels of 6, 7, and 8; and, finally, reaction temperatures of 273 K, 283 K, 288 K, 295 K, and 303 K were tested. Trials were repeated in doublets, with additional trials performed as necessary in order to ensure consistency. The reusability/stability of the Pt-MCM catalyst was tested by using the same amount of catalyst in five subsequent hydrolysis reactions. At the beginning of

each new trial, 0.00095 mol of $NaBH_4$ reactant was added. The reaction conditions were kept constant at ambient conditions (pH 7 and 295 K).

3.1. Catalyst Characterization

Figure 1 depicts TEM images of the Pt-MCM composite. Figure 1a,b clearly show the presence of nanoparticles dispersed across the MCM support. Figure 1c allows the size of a few nanoparticles to be determined to be 1–7 nm in diameter, with an average particle size of 3.51 nm in diameter. In comparison with Figure 1a, some variety in NP size can be seen, allowing the size of the NPs to be considered from 2 to 10 nm in general.

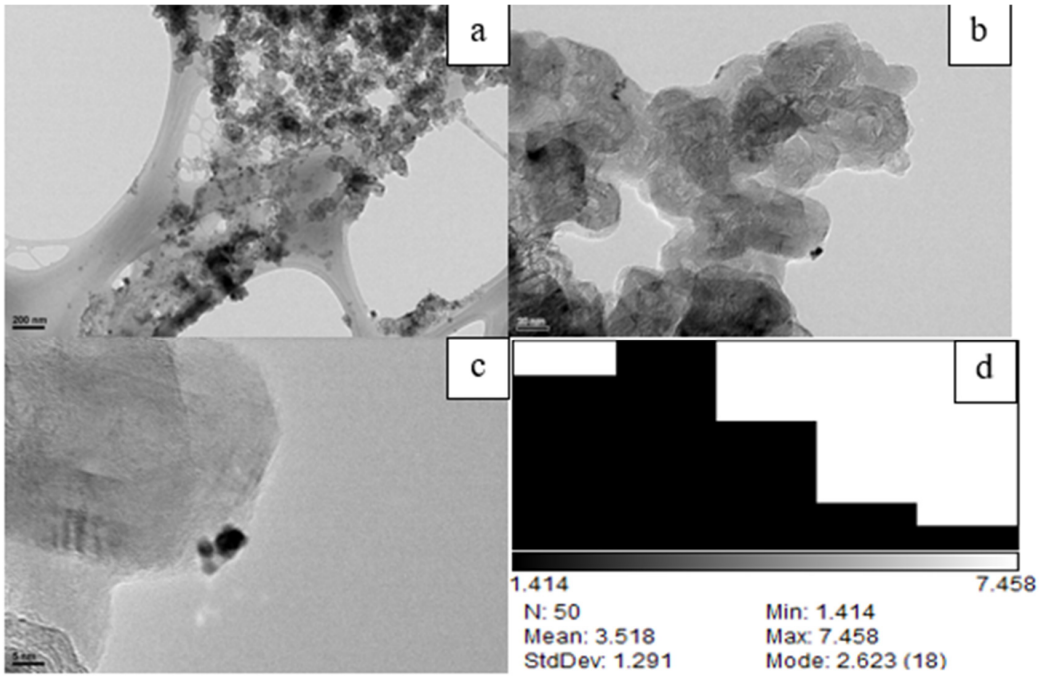


Figure 1. TEM images of the Pt-MCM catalyst at magnifications of (**a**) 200 nm, (**b**) 20 nm, and (**c**) 5 nm. (**d**) is a particle size distribution histogram for 50 measured particles.

Through the use of SEM (Figure 2a), it was determined that the synthesized PtNPs were even smaller than initially thought, with some appearing to be 1 nm or less. EDS scans of the nanoparticles confirmed their identity to be platinum with 0.6% loading (Figure 2b).

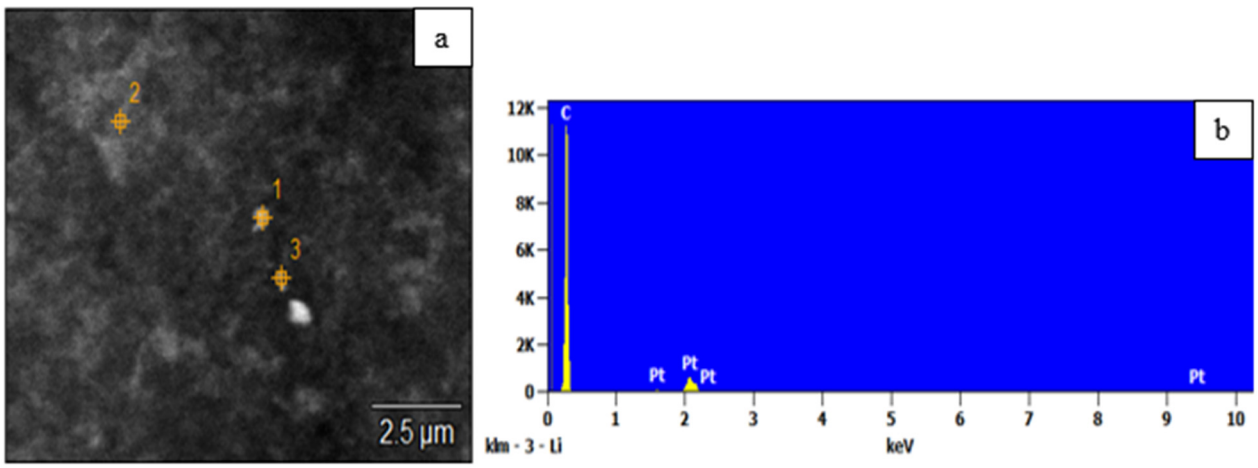


Figure 2. (**a**): SEM micrograph of the Pt-MCM composite with a scale of 2.5 nm. (**b**): EDS spectrum of the Pt-MCM composite in (**a**) and the yellow marks 1, 2 and 3 are the locations used to generate the EDS measurements in (**a**).

The XRD spectra of the catalyst are shown in Figure 3. A large peak indicative of the MCM backbone is seen in both the pure MCM and the Pt-MCM composite. The peaks between 20 °C and 30 °C are often seen in carbon-based materials due to graphitic characteristics. There is a shift in this peak after the incorporation of nanoparticles that has been previously reported in similar materials and can be attributed to a change in the lattice structure of the MCM material due to nanoparticles adhering to it [30]. Two peaks indicative of PtNPs can be seen at 39.9° and 42.8°, representing the (1 1 1) and (2 0 0) faces of the face-centered cubic (FCC) structured nanoparticles (ICDD PDF 70-2431) [31]. There are three other peaks associated with FCC structures that were not seen; however, this is most likely due to the limitations of the instrument that struggled to detect the small particles.

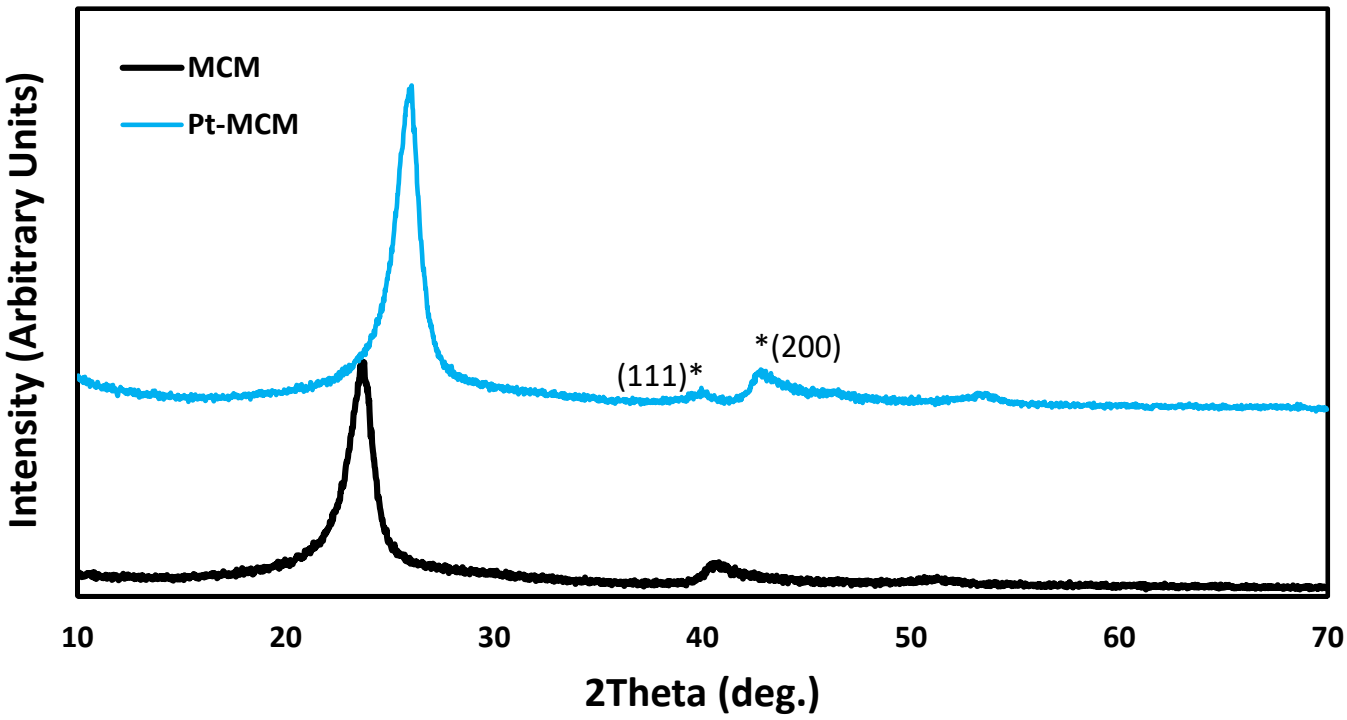


Figure 3. XRD spectra for the Pt-MCM catalyst.

3.2. Catalytic Trials

The results of the catalytic ability of Pt-MCM under different quantities of $NaBH_4$ are shown in Figure 4. For consistency, the temperature of all trials was kept at ambient conditions (295 K and pH 7). The catalyst was first tested against an $NaBH_4$ quantity of 0.00079 mol. This reaction was run for two hours, producing 23.9 mL of hydrogen on average. When tested at 0.00095 mol, the produced hydrogen was determined to be 35.6 mL. The final quantity was tested was 0.0011 mol, which produced roughly 48.4 mL. These volumes can be divided by the reaction time and the amount of catalyst used to calculate both the rate of hydrogen generation and the turnover number (TON). For the given experiments, the rates of hydrogen generation and the corresponding TONs are as follows: for 0.00079 mol of $NaBH_4$, the hydrogen generation rate was 0.0199 mL min^{-1} mg^{-1} with a TON of 33.4; for 0.00095 mol of $NaBH_4$, the hydrogen generation rate was 0.0298 mL min^{-1} mg^{-1} with a TON of 49.7; and for 0.0011 mol of $NaBH_4$, the hydrogen generation rate was 0.04036 mL min^{-1} mg^{-1} with a TON of 49.67. The hydrogen generation rate represents the volume of hydrogen gas produced per minute per milligram of catalyst, reflecting the catalyst's efficiency in facilitating the hydrolysis reaction. The TON quantifies the catalytic activity in terms of the number of moles of hydrogen produced per mole of catalyst over the course of the reaction, indicating the efficiency of the catalyst in generating hydrogen per active site.

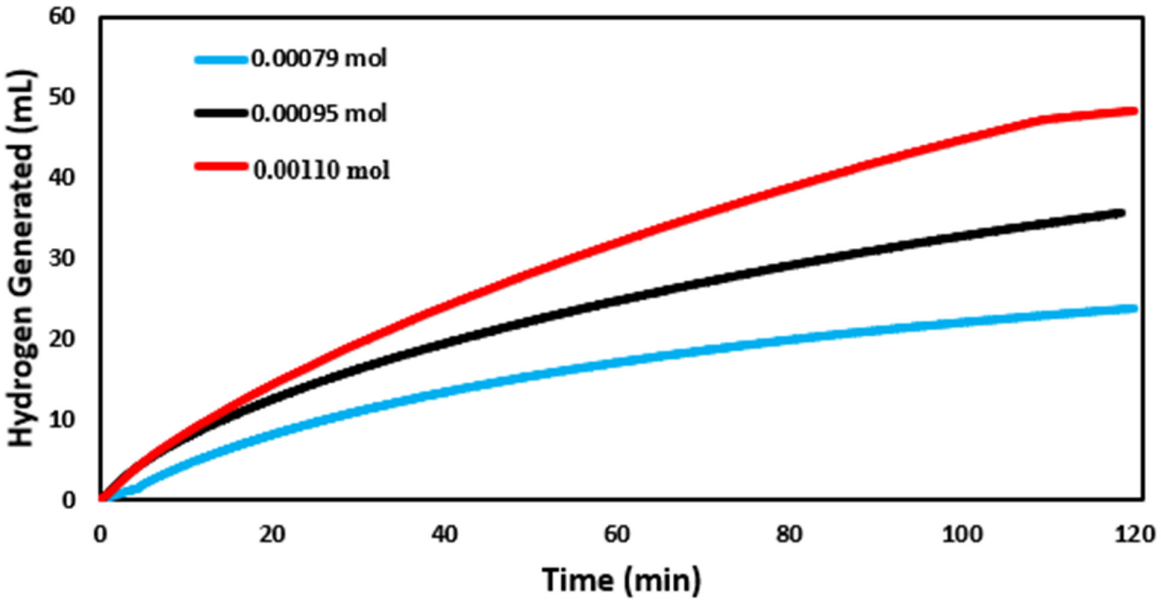


Figure 4. Volume of hydrogen generated versus time in minutes with the Pt-MCM catalyst when varying $NaBH_4$ quantity.

The pH of the reaction was adjusted to see how it would affect the catalyst, as seen in Figure 5. For comparison purposes, the quantity of $NaBH_4$ was kept consistent at 0.00095 mol and temperature was kept at 295 K. Since the previous study already included trials tested at pH 7 and 0.00095 mol, this became the baseline for comparison. First, the pH of the reaction was lowered to pH 6, resulting in an increased hydrogen production over pH 7 and an average amount of generated hydrogen of 54.7 mL. When the pH of the reaction was raised to pH 8, the volume of produced hydrogen was reduced to 25.7 mL. As before, these volumes allowed for the hydrogen generation rates to be calculated at 0.0456 mL min^{-1} mg^{-1} and 0.0214 mL min^{-1} mg^{-1} for pH 6 and 7, respectively. These results are supported by previously reported studies. It has been observed that at higher pH levels, the increased concentration of OH^- ions may compete for released hydrogen [32,33]. Conversely, the increased concentration of H^+ ions in acidic solutions may facilitate the splitting of a hydrogen off water molecules [34].

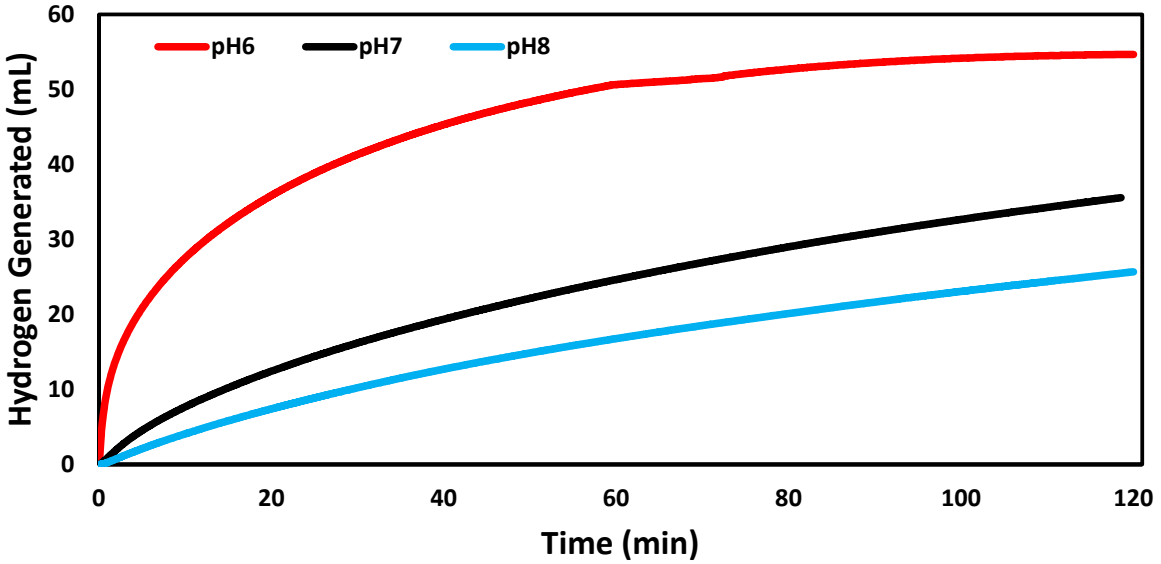


Figure 5. Volume of hydrogen generated versus time in minutes with the Pt-MCM catalyst when varying pH conditions.

Figure 6 shows the results of the Pt-MCM catalyst when tested at varying temperatures. To maintain consistency, all trials were run using 0.00095 mol of $NaBH_4$ and a pH of 7. As in the case of the pH study, since 0.00095 mol, pH 7, and 295 K had already been tested, these conditions became the point for comparison. Temperature trials began with the lowering the temperature of the reaction to 275 K. At this temperature, the produced hydrogen was observed to be 8.9 mL. When the reaction was lowered to 283 K, roughly 18.6 mL of hydrogen was produced. Next, a volume of 23.5 mL was produced when the reaction temperature was lowered to 288 K. Finally, the catalytic ability of the Pt-MCM catalyst was tested under increased temperature conditions. At 303 K, the amount of generated hydrogen was discovered to be 44.9 mL. The rates of the reaction at each of these temperatures was then calculated for 273 K, 283 K, 288 K, and 303 K to be 0.0074 mL min^{-1} mg^{-1}, 0.0155 mL min^{-1}, mg^{-1} 0.0196 mL min^{-1} mg^{-1}, and 0.0374 mL min^{-1} mg^{-1}, respectively.

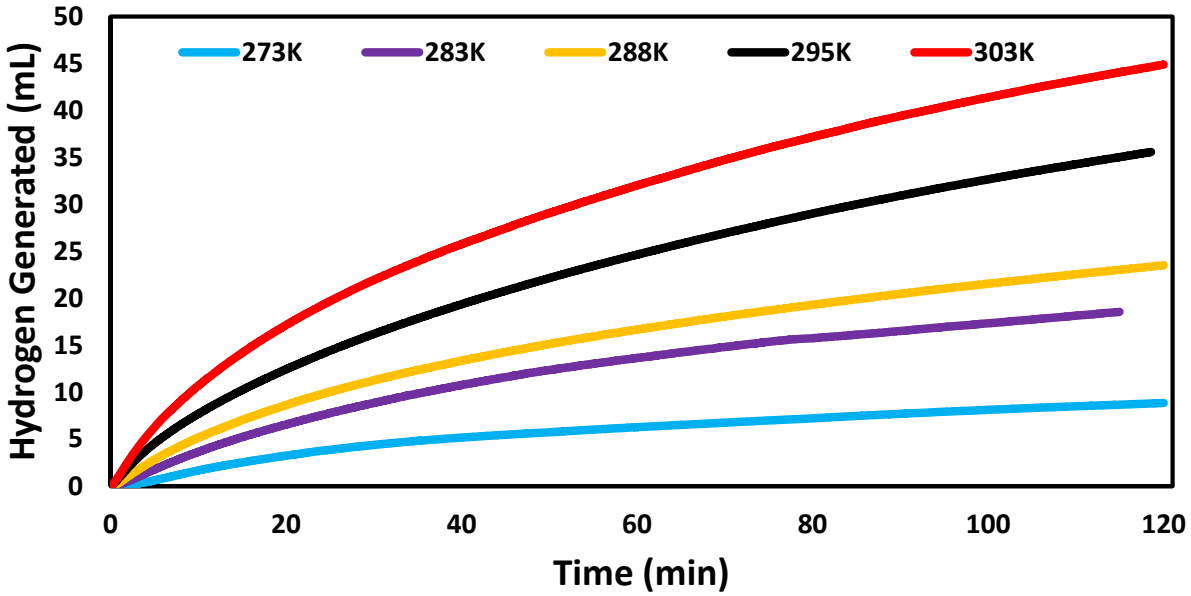


Figure 6. Volume of hydrogen generated versus time in minutes with the PtNP–MCM catalyst when varying temperatures.

Several trends can be noticed by observing Figures 4–6 that give information on optimal conditions for this hydrolysis reaction. It is clear that increasing the quantity of $NaBH_4$ results in an increase in hydrogen generation rate (Figure 4). This was expected, as Le Chatelier's principle states that increasing the quantity of a reactant will result in an increase in the quantity of the product (Equation (1)). As described above, when testing the pH of the reaction (Figure 5), it was observed that lowering the pH of the solution increased the reaction rate and the opposite was true for raising the pH. In one of the earliest studies on this reaction, the team of Schlesinger et al. (1953) stated that lowering the pH of this reaction results in an increase in the formation of the borate ions that then release hydrogen [34]. Another early study by the team of Kaufman et al. (1985) found that increasing the pH of this reaction has detrimental effects, possibly due to an increase viscosity of the reaction solution [33]. This temperature study (Figure 6) shows that heating the reaction is beneficial and cooling it is detrimental to the hydrogen generation rates. Based on Equation (1), this reaction must be endothermic in this case. All these results were consistent with the previous work of this team on this reaction [15–19].

The reaction rates used to create this Arrhenius plot (Figure 7) stemmed from the Arrhenius Equation (2).

$$\ln k = -\frac{Ea}{RT} + \ln A \quad (2)$$

where the variables in (2) represent the following: k is the reaction rate at each studied temperature, Ea is the activation energy of the reaction measured in kJ per mol, R is the universal gas constant, T is the absolute temperature measured in Kelvin, and, lastly, A is the pre-exponential factor. This equation allowed for Figure 7 to be created, and from this plot, the equation of the line could be determined. The inverse slope of this equation multiplied by the gas constant allowed the activation energy of the reaction as catalyzed by Pt-MCM to be determined as 37.7 kJ mol^{-1}.

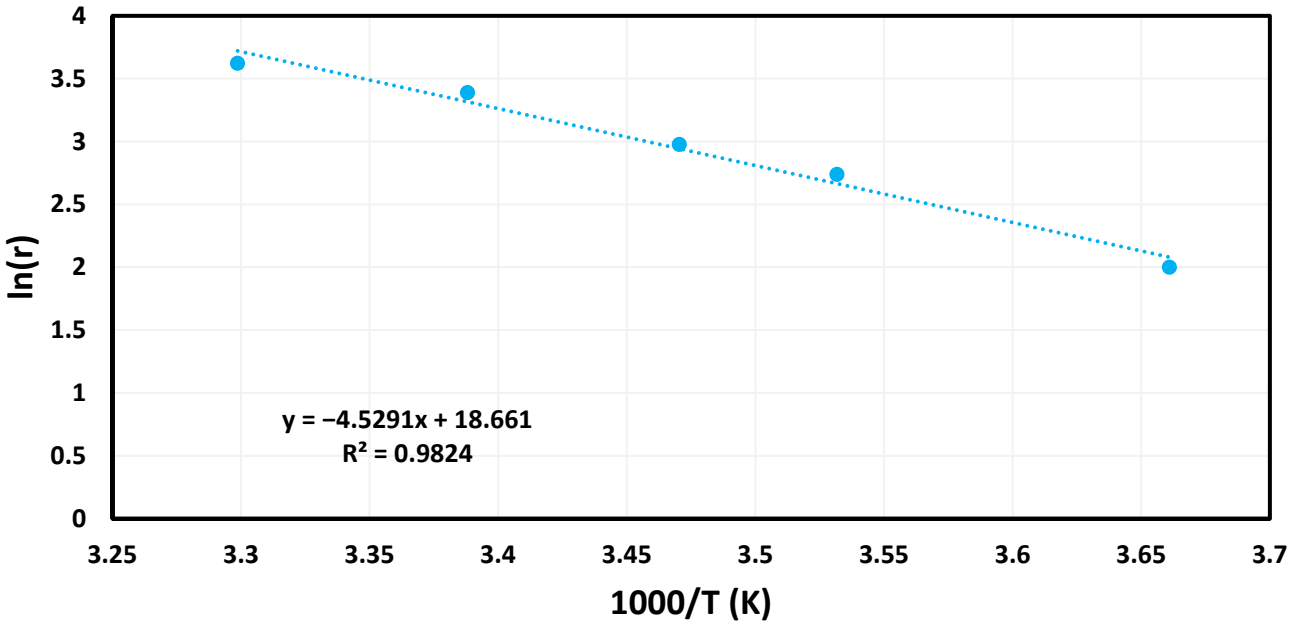


Figure 7. Arrhenius plot for calculating the activation energy of a hydrogen generation reaction for the Pt-MCM catalyst.

When Pt-MCM was compared with similar catalysts for the hydrolysis of $NaBH_4$, (Table 1), it showed a competitive advantage. Compared with unsupported nanoparticles like BCD-AuNP and PtNPs, this catalyst was superior to both, indicating that the addition of the MCM support improved the catalytic ability. When compared with other composites using carbon-based supports, this catalyst was superior to all but gold nanoparticles on multiwalled carbon nanotubes (AuMWCNTs) and Pt-Pd/CNTs, both of which have incredibly low Ea values of 21.1 kJ mol^{-1} and 19 kJ mol^{-1}, respectively. Pt-MCM still holds an advantage over these catalysts as the MCM backbone is derived from corn starch, whereas MWCNTs and CNTs require extreme temperatures and/or harsh chemicals. The PtNPs supported over the MCM have a lower activation energy than other nanoparticles supported over graphene-like materials (GLMs) and fused carbon spheres (FCS).

Table 1. Comparison of reported activation energies for catalyzed $NaBH_4$ hydrolysis.

Catalyst	Activation Energy (kJ mol^{-1})	Reaction Conditions (K)	Ref.
BCD-AuNP	54.7	283–303	[18]
PtNPs	39.2	283–303	[19]
Pd/C	28	298–328	[35]
Pt–Pd/CNTs	19	302–332	[36]
AuMWCNTs	21.1	273–303	[16]
Ag/MWCNTs	44.5	273–303	[37]
Pd/MWCNTs	62.7	273–303	[38]

Table 1. *Cont.*

Catalyst	Activation Energy (kJ mol^{-1})	Reaction Conditions (K)	Ref.
PtMWCNTs	46.2	283–303	[39]
CuGLM	46.8	283–303	[40]
AuFGLM	45.5	283–303	[41]
PdFGLM	45.1	283–303	[42]
PtFCS	53.0	283–303	[43]
Pt-MCM	37.7	273–303	This Work

3.3. Reusability Tests

Five consecutive reusability trials were performed on the catalyst to evaluate its performance over multiple uses. The reaction conditions for these trials were standardized as follows: 0.00095 moles of sodium borohydride ($NaBH_4$) were used, with the pH of the solution maintained at 7 and the reaction temperature kept constant at 295 K. As evident in Figure 8, there was a notable decline in the amount of hydrogen gas produced after the first trial. This decrease can be attributed to the reduction in catalyst activity over time. Several factors may have contributed to this decline, including surface changes due to the formation of BO_2^- (as described in Equation (1)) and structural changes to the catalyst. These changes reduced the number of active sites available for the hydrolysis reaction, resulting in lower hydrogen production. Additionally, the deposition of BO_2 can alter the optimal ratio between a catalyst and its support material, further decreasing catalyst activity [44]. Following the initial drop in hydrogen production after the first trial, the amount of generated hydrogen gas began to stabilize. This stabilization was likely due to the aforementioned compensatory mechanisms coming into effect, maintaining a more consistent level of catalyst activity despite the initial loss. Over the subsequent trials, the catalyst produced an average volume of 20.3 mL of hydrogen gas, indicating that although there was an initial decline, the catalyst maintained a relatively stable performance in the later trials.

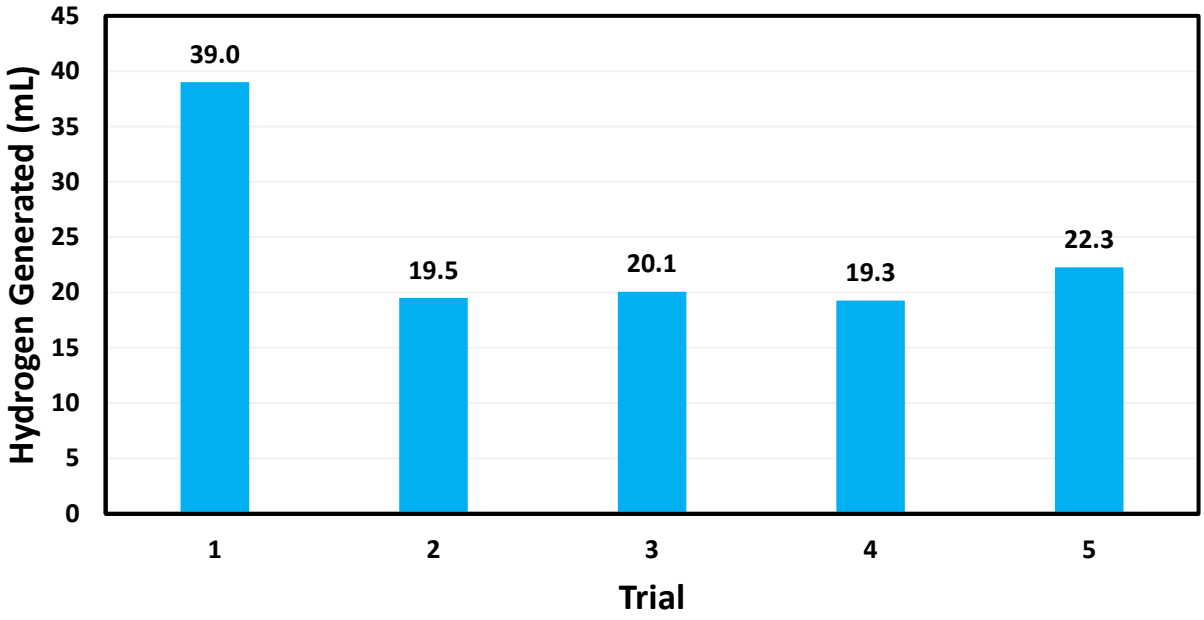
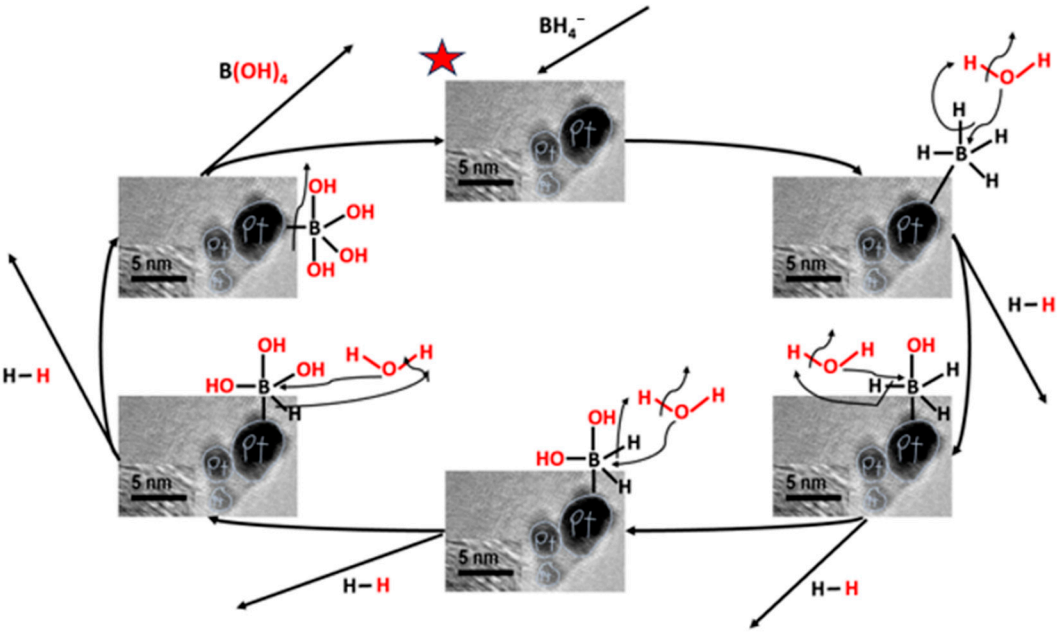


Figure 8. Testing reusability of the Pt-MCM catalyst.

The proposed method of hydrogen generation in the hydrolysis of $NaBH_4$ as catalyzed by Pt-MCM is depicted in Scheme 1. The reaction begins with a single borohydride ion

(BH_4^-) attacking and fixing itself to a platinum nanoparticle on the MCM backbone. A nearby water molecule is attracted to the borohydride, attacking it and attaching itself. This causes a hydrogen from the borohydride to be forced off, which attacks a single hydrogen from the water molecule, splitting it off. This process causes a single H_2 molecule to be produced, and a hydroxyl group is left in the place of the hydrogen on the borohydride. This process can happen three more times, after which the $B(OH)_4$ molecule separates from the PtNP, allowing a new borohydride to replace it and the process to repeat. Each time the cycle completes, 4 H_2 molecules are produced [45].



Scheme 1. Theorized method of hydrogen generation as catalyzed by Pt-MCM. The cycle begins at the top of the scheme, marked by a star.

4. Conclusions

An MCM material derived from starch and a platinum nanoparticle nanocomposite catalyst was synthesized and characterized. TEM results showed the presence of both the MCM and platinum nanoparticles and their attachment. SEM/EDS and XRD showed the presence of a platinum metal composite. As evident in the catalytic data, the nanocomposite catalyst produced more hydrogen gas at increasing $NaBH_4$ quantities, acidic conditions, and higher temperatures. The activation energy was determined to be 37.7 kJ mol^{-1}. The results of the reusability trials showed that the catalyst became stable after the first trial and could consistently produce hydrogen. These results indicate that platinum nanoparticles supported on an MCM framework can serve as an effective catalyst for the production of hydrogen gas. Their catalytic activity, along with their sustainability and low cost of production, make this catalyst an important contribution to help curb the continued use of non-renewable energy sources.

Author Contributions: Methodology, T.M.A.-F.; Validation, T.M.A.-F.; Formal analysis, E.B., Q.Q. and T.M.A.-F.; Investigation, Q.Q.; Resources, T.M.A.-F.; Data curation, E.B.; Writing—original draft, E.B.; Writing—review & editing, Q.Q. and T.M.A.-F. All authors have read and agreed to the published version of the manuscript.

Funding: This research received no external funding.

Data Availability Statement: The raw data supporting the conclusions of this article will be made available by the authors on request.

Acknowledgments: The corresponding author acknowledges Lawrence J. Sacks' professorship in chemistry.

Conflicts of Interest: The authors declare no conflicts of interest.

References

1. Allister, D. *The Heat Is On: Taking Stock of Global Climate Ambition*; NDC Global Outlook Report 2019; UNDP: New York, NY, USA, 2019; p. 13. Available online: https://unfccc.int/sites/default/files/resource/NDC%20Outlook.pdf (accessed on 19 June 2024).
2. Veziroglu, T.N. 21st Century's Energy: Hydrogen Energy System. In *Assessment of Hydrogen Energy for Sustainable Development*; Springer: Dordrecht, The Netherlands, 2007; pp. 9–31. [CrossRef]
3. Rivkin, C.; Burgess, R.; Buttner, W. *Hydrogen Technologies Safety Guide*; National Renewable Energy Lab.: Golden, CO, USA, 2015. [CrossRef]
4. Yang, W.; Chen, S. Recent progress in electrode fabrication for electrocatalytic hydrogen evolution reaction: A mini review. *Chem. Eng. J.* **2020**, *393*, 124726. [CrossRef]
5. Abdelghafar, F.; Xu, X.; Jiang, S.P.; Shao, Z. Designing single-atom catalysts toward improved alkaline hydrogen evolution reaction. *Mater. Rep. Energy* **2022**, *2*, 100144. [CrossRef]
6. Jin, C.; Huo, L.; Tang, J.; Li, S.; Jiang, K.; He, Q.; Dong, H.; Gong, Y.; Hu, Z. Precise Atomic Structure Regulation of Single-Atom Platinum Catalysts toward Highly Efficient Hydrogen Evolution Reaction. *Small* **2023**, *20*, 2309509. [CrossRef] [PubMed]
7. Yang, J.; Yang, Z.; Li, J.; Gang, H.; Mei, D.; Yin, D.; Deng, R.; Zhu, Y.; Li, X.; Wang, N.; et al. Engineering a hollow bowl-like porous carbon-confined Ru–MgO hetero-structured nanopair as a high-performance catalyst for ammonia borane hydrolysis. *Mater. Horiz.* **2024**, *11*, 2032–2040. [CrossRef] [PubMed]
8. Zhang, J.; Lu, H.; He, P.; Ren, Z.; Shen, G.; Liu, R.; Wang, L.; Luo, G. The performance and corrosion resistance of an electrodeposited Ni-Mo-Cu HER catalyst. *Surf. Coat. Technol.* **2023**, *465*, 129596. [CrossRef]
9. Demirci, U.B.; Miele, P. Sodium borohydride versus ammonia borane, in hydrogen storage and direct fuel cell applications. *Energy Environ. Sci.* **2009**, *2*, 627. [CrossRef]
10. Liang, C.; Li, Z.; Dai, S. Mesoporous Carbon Materials: Synthesis and Modification. *Angew. Chem. Int.* **2008**, *47*, 3696–3717. [CrossRef]
11. Horváth, E.; Puskás, R.; Rémiás, R.; Mohl, M.; Kukovecz, Á.; Kónya, Z.; Kiriesi, I. A Novel Catalyst Type Containing Noble Metal Nanoparticles Supported on Mesoporous Carbon: Synthesis, Characterization and Catalytic properties. *Top. Catal.* **2009**, *52*, 1242–1250. [CrossRef]
12. Xia, Y.; Mokaya, R. Generalized and Facile Synthesis Approach to N-Doped Highly Graphitic Mesoporous Carbon Materials. *Chem. Mater.* **2005**, *17*, 1553–1560. [CrossRef]
13. Su, F.; Zeng, J.; Bao, X.; Yu, Y.; Lee, J.Y.; Zhao, X.S. Preparation and Characterization of Highly Ordered Graphitic Mesoporous Carbon as a Pt Catalyst Support for Direct Methanol Fuel Cells. *Chem. Mater.* **2005**, *17*, 3960–3967. [CrossRef]
14. Chang, H.; Joo, S.H.; Pak, C. Synthesis and characterization of mesoporous carbon for fuel cell applications. *J. Mater. Chem.* **2007**, *17*, 3078–3088. [CrossRef]
15. Abdel-Fattah, T.; Wixtrom, A. Catalytic Reduction of 4-Nitrophenol Using Gold Nanoparticles Supported on Carbon Nanotubes. *ECS J. Solid State Sci. Technol.* **2014**, *3*, M18–M20. [CrossRef]
16. Huff, C.; Dushatinski, T.; Barzanji, A.; Abdel-Fattah, N.; Barzanji, K.; Abdel-Fattah, T.M. Pretreatment of Gold Nanoparticle Multi-Walled Carbon Nanotube Composites for Catalytic Activity toward Hydrogen Generation Reaction. *ECS J. Solid State Sci. Technol.* **2017**, *6*, 69–71. [CrossRef]
17. Dushatinski, T.; Huff, C.; Abdel-Fattah, T.M. Characterization of electrochemically deposited films from aqueous and ionic liquid cobalt precursors toward hydrogen evolution reactions. *Appl. Surf. Sci.* **2016**, *385*, 282–288. [CrossRef]
18. Quach, Q.; Biehler, E.; Elzamzami, A.; Huff, C.; Long, J.M.; Abdel-Fattah, T.M. Catalytic Activity of Beta-Cyclodextrin-Gold Nanoparticles Network in Hydrogen Evolution Reaction. *Catalysts* **2021**, *11*, 118. [CrossRef]
19. Huff, C.; Biehler, E.; Quach, Q.; Long, J.M.; Abdel-Fattah, T.M. Synthesis of highly dispersive platinum nanoparticles and their application in a hydrogen generation reaction. *Colloid Surf. A* **2021**, *610*, 125734. [CrossRef]
20. Antolini, E. Formation, microstructural characteristics and stability of carbon supported platinum catalysts for low temperature fuel cells. *J. Mater. Sci.* **2003**, *38*, 2995–3005. [CrossRef]
21. Liu, J.; Zhou, Z.; Zhao, X.; Xin, Q.; Sun, G.; Yi, B. Studies on performance degradation of a direct methanol fuel cell (DMFC) in life test. *Phys. Chem. Chem. Phys.* **2004**, *6*, 134. [CrossRef]
22. Hotze, E.M.; Phenrat, T.; Lowry, G.V. Nanoparticle Aggregation: Challenges to Understanding Transport and Reactivity in the Environment. *J. Environ. Qual.* **2010**, *39*, 1909. [CrossRef]
23. Periana, R.A.; Taube, D.J.; Gamble, S.; Taube, H.; Satoh, T.; Fujii, H. Platinum Catalysts for the High-Yield Oxidation of Methane to a Methanol Derivative. *Science* **1998**, *24*, 560–564. [CrossRef]
24. Sabourault, N.; Mignani, G.; Wagner, A.; Mioskowski, C. Platinum Oxide (PtO_2): A Potent Hydrosilylation Catalyst. *Org. Lett.* **2002**, *4*, 2117–2119. [CrossRef]
25. Ely, J.C.; Neal, C.R.; Kulpa, C.F.; Schneegurt, M.A.; Seidler, J.A.; Jain, J.C. Implications of Platinum-Group Element Accumulation along U.S. Roads from Catalytic-Converter Attrition. *Environ. Sci. Technol.* **2001**, *35*, 3816–3822. [CrossRef] [PubMed]
26. Abu-Reziq, R.; Wang, D.; Post, M.; Alper, H. Platinum Nanoparticles Supported on Ionic Liquid-Modified Magnetic Nanoparticles: Selective Hydrogenation Catalysts. *Adv. Synth. Catal.* **2007**, *349*, 2145–2150. [CrossRef]

27. Fang, B.; Chaudhari, N.K.; Kim, M.-S.; Kim, J.H.; Yu, J.-S. Homogeneous Deposition of Platinum Nanoparticles on Carbon Black for Proton Exchange Membrane Fuel Cell. *J. Am. Chem. Soc.* **2009**, *131*, 15330–15338. [CrossRef]
28. Su, C.; Yang, T.; Zhou, W.; Wang, W.; Xuc, X.; Shao, Z. Pt/C–$LiCoO_2$ composites with ultralow Pt loadings as synergistic bifunctional electrocatalysts for oxygen reduction and evolution reactions *J. Mater. Chem. A* **2016**, *4*, 4516–4524. [CrossRef]
29. Biehler, E.; Quach, Q.; Abdel-Fattah, T. Screening study of Different Carbon Based Materials for Hydrogen. *ECS J. Solid State Sci. Technol.* **2023**, *12*, 081002. [CrossRef]
30. Antolini, E.; Cardellini, F. Formation of carbon supported PtRu alloys: An XRD analysis. *J. Alloys Compd.* **2001**, *315*, 118–122. [CrossRef]
31. Karthik, R.; Sasikumar, R.; Chen, S.-M.; Govindasamy, M.; Vinoth Kumar, J.; Muthuraj, V. Green Synthesis of Platinum Nanoparticles Using Quercus Glauca Extract and Its Electrochemical Oxidation of Hydrazine in Water Samples. *Int. J. Electrochem. Sci.* **2016**, *11*, 8245–8255. [CrossRef]
32. Grzeschik, R.; Schäfer, D.; Holtum, T.; Küpper, S.; Hoffmann, A.; Schlücker, S. On the Overlooked Critical Role of the pH Value on the Kinetics of the 4-Nitrophenol NaBH4-Reduction Catalyzed by Noble Metal Nanoparticles (Pt, Pd, Au). *J. Phys. Chem. C* **2020**, *124*, 2939–2944. [CrossRef]
33. Kaufman, C.M.; Sen, B. Hydrogen Generation by Hydrolysis of Sodium Tetrahydroborate: Effects of Acids and Transition Metals and Their Salts. *J. Chem. Soc. Dalton Trans.* **1985**, *2*, 307–313. [CrossRef]
34. Schlesinger, H.I.; Brown, H.C.; Finholt, A.E.; Gilbreath, J.R.; Hoekstra, H.R.; Hyde, E.K. Sodium borohydride, its hydrolysis and its use as a reducing agent and in the generation of hydrogen. *J. Am. Chem. Soc.* **1953**, *75*, 215–219. [CrossRef]
35. Patel, N.; Patton, B.; Zanchetta, C.; Fernandes, R.; Guella, G.; Kale, A.; Miotello, A. Pd-C power and thin film catalysts for hydrogen production by hydrolysis of sodium borohydride. *Int. J. Hydrogen Energy* **2008**, *33*, 287–292. [CrossRef]
36. Peña-Alonso, R.; Sicurelli, A.; Callone, E.; Carturan, G.; Raj, R. A picoscale catalyst for hydrogen generation from $NaBH_4$ for fuel cells. *J. Power Sources* **2007**, *165*, 315–323. [CrossRef]
37. Huff, C.; Long, J.M.; Aboulatta, A.; Heyman, A.; Abdel-Fattah, T.M. Silver Nanoparticle/Multi-Walled Carbon Nanotube Composite as Catalyst for Hydrogen Production. *ECS J. Solid State Sci. Technol.* **2017**, *6*, 115–118. [CrossRef]
38. Huff, C.; Long, J.M.; Heyman, A.; Abdel-Fattah, T.M. Palladium Nanoparticle Multiwalled Carbon Nanotube Composite as Catalyst for Hydrogen Production by the Hydrolysis of Sodium Borohydride. *ACS Appl. Energy Mater.* **2018**, *1*, 4635–4640. [CrossRef]
39. Huff, C.; Quach, Q.; Long, J.M.; Abdel-Fattah, T.M. Nanocomposite Catalyst Derived from Ultrafine Platinum Nanoparticles and Carbon Nanotubes for Hydrogen Generation. *ECS J. Solid State Sci. Technol.* **2020**, *9*, 101008. [CrossRef]
40. Quach, Q.; Biehler, E.; Abdel-Fattah, T.M. Synthesis of Copper Nanoparticles Supported over Graphene-like Material Composite as a Catalyst for Hydrogen Evolution. *J. Compos. Sci.* **2023**, *7*, 279. [CrossRef]
41. Biehler, E.; Quach, Q.; Abdel-Fattah, T.M. Gold Nanoparticles AuNP Decorated on Fused Graphene-like Materials for Application in a Hydrogen Generation. *Materials* **2023**, *16*, 4779. [CrossRef]
42. Quach, Q.; Biehler, E.; Abdel-Fattah, T.M. Synthesis of Palladium Nanoparticles Supported over Fused Graphene-like Material for Hydrogen Evolution Reaction. *Catalysts* **2023**, *13*, 1117. [CrossRef]
43. Biehler, E.; Quach, Q.; Abdel-Fattah, T.M. Synthesis of Platinum Nanoparticles Supported on Fused Nanosized Carbon Spheres Derived from Sustainable Source for Application in a Hydrogen Generation Reaction. *Nanomaterials* **2023**, *13*, 1994. [CrossRef]
44. Bilen, M.; Guru, M.; Cakanyildirim, C. Role of NaCl in NaBH4 production and its hydrolysis. *Energy Convers. Manag.* **2013**, *72*, 134–140. [CrossRef]
45. Abdel-Fattah, T.M.; Biehler, E. Carbon Based Supports for Metal Nanoparticles for Hydrogen Generation Reactions Review. *Adv. Carbon J.* **2024**, *1*, 1–19. [CrossRef]

Disclaimer/Publisher's Note: The statements, opinions and data contained in all publications are solely those of the individual author(s) and contributor(s) and not of MDPI and/or the editor(s). MDPI and/or the editor(s) disclaim responsibility for any injury to people or property resulting from any ideas, methods, instructions or products referred to in the content.